A Study of an Excellent Input Prediction Method Based on the Kalman Filter, Combined with Experimental Verification for a Superquick Heat Flux in a Igniter Stick

Yang-Hsiung Ko

Department of Power Vehicle and Systems Engineering,
Chung Cheng Institute of Technology,
National Defense University

ABSTRACT

Igniter stick transient ignition will generate soaring temperature jet flows from vent holes that oblige special design effects for an explosive. The *excellent input prediction method* (EIPM) can be useful to the inverse heat transfer conduction problem in estimating the unknown instantaneous time-varying heat flux of the igniter stick as presented in this study. An EIPM is created with both the Kalman filter and the recursive least squares estimator are used to predict the unknown *superquick heat flux* （SHF）from the transient temperature data from a thin copper plate at the rear of the igniter stick. The Kalman filter can inversely estimate the unknown heat source strength using the measured temperature on the outer surface. The recursive least squares estimator uses the residual innovation sequence from the filter to recursively compute the magnitude of the unknown SHF. The prediction authority is caused by the temperature measurements of copper plates with different thicknesses, sampling time interval, space discrete interval, weighting factor and the processing noise covariance. The results show that the EIPM is active and powerful in estimating the unknown SHF of the igniter stick.

Keywords: temperature, heat flux, igniter stick

建構在卡爾曼濾波上之智能輸入法估算傳火管瞬發熱通量及其實驗驗證

葛揚雄

國防大學理工學院動力及系統工程學系

摘　　要

傳火管點燃瞬間產生之高溫噴流對點火藥之溫度分佈將影響火藥鏈之設計，本研究顯示智能輸入估算法可有效估算逆向熱傳問題中傳火管未知瞬發時變熱通量。智能輸入估算法由卡爾曼濾波器（Kalman filter）及遞迴式最小平方估測器兩者組成，由薄銅片上之背面暫態溫度數據用來預估傳火管未知瞬發熱通量。卡爾曼濾波器藉由外部表面之量測溫度，可逆向估算未知熱源強度；遞迴式最小平方估測器則藉由濾波器產生之剩餘值更新序列遞迴地計算輸入系統之傳火管未知瞬發熱通量。估算準據受不同厚度銅片溫度、取樣時間間隔、空間離散間隔、權重因子及程序誤差變異量等影響。結果顯示智能輸入估算法可強速估算傳火管未知瞬發熱通量。

關鍵詞：溫度，熱通量，傳火管

文稿收件日期 100.1.6;文稿修正後接受日期 100.4.25; *通訊作者
Manuscript received January 6, 2011; revised March 25, 2011; * Corresponding author

Ⅰ. INTRODUCTION

The primer cap and the black powder charge are usually assembled in a igniter stick (Fig. 1). The igniter stick used in the cartridge

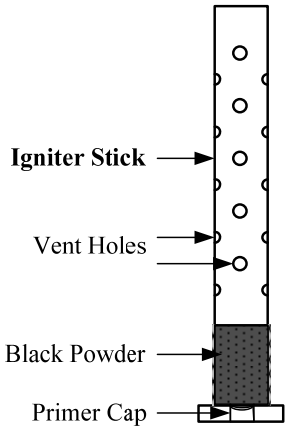

Fig.1. A igniter stick.

case contains sufficient black powder to properly ignite the material in the cartridge case. Those used with separate loaded propelling charges contain only enough black powder to ignite the igniter charge attached to the propelling charge. Igniting materials must be ignited using high temperature because the latter may effect detonations. The heat must flow from the hot igniter stick flame to the material grain. This sensible heat, plus that due to any adiabatic gas compression in the vicinity, is the sole source of heat available to uniformly ignite the propellant. Heat flow to the next charge occurs by radiation and conduction. The net radiation surrounds one body and the other in the case. Luminous flames which contain large numbers of solid particles in suspension radiate much more intensely than non-luminous flames. This accounts in large measure for the superiority of black powder for use in primers because the explosion products contain large amounts of solids such as potassium carbonate and sulfate, which radiate intense heat, in contrast to the non-luminous flames from smokeless powders.

Substantial theories of the inverse heat conduction problems have been developed and applied in recent years in the heat transfer field [1-3]. Yu [4] used the lagrangian analysis of continua to analyze the heat conduction mechanism under the fixed temperature boundary condition. Hon [5] analyzed it by using the fixed flux control instead of the fixed temperature boundary condition and showed the precision in measuring the physical condition. Though their universe regularization method is simpler, it produces higher computational load due to the longer solving time and the increasing number of matrix dimensions. The conjugate gradient iteration method adopts the control concept to solve the inverse heat conduction problem and has the computational structure with higher efficiency. This method was adopted by many researchers such as Huang [6] and Li [7]. Both algorithms are the batch type of off-line processes which are not very efficient. Meng [8] presented a modified input estimation method for tracking a maneuvering target. Scarpa and Milano [9] applied the Kalman smoothing technique in inverse heat transfer estimation and accurate results were obtained. Polat [10] used the wall function and the corrected presentation of the shearing stress to explain the influences on material conduction on impact surfaces. Linton and Agonafer [11] utilized the software applied to calculate the fluid dynamic problems to explore the heat-conducting phenomenon on a flat type plate. They compared the simulated results with results from actual experiments. Sathe [12] made use of the numerical simulation method to investigate the flow field and heat transfer by conduction on vertical square-column fins under the impact-emitting flow cooling process. Jonsson and Palm [13] found that the heat resistance value was estimated using the empirical formula from the actual experiment. Maveety and Jung [14] used several flow fields with different Reynolds number values to conduct numerical simulations and compare the results with experimental results. In the practical use, the parameters should be determined in real time.

The EIPM is composed of the Kalman filter and the recursive least square estimator. The Kalman filter produces a residual renewal array. The array is applied to the least square estimator to estimate the parameters. In view of the fact that each estimate only requires the output and measurement of the last moment, it will greatly reduce the computational memory burden. The EIPM is an on-line recursive input estimation algorithm that can efficiently and accurately estimate the time-varying unknown inputs. The amount of heat coming along with rapid igniter stick combustion will expand rapidly. The temperature strength can be estimated when the SHF produced by the igniter stick can be sufficiently measured in real time. The study proposes EIPM to estimate the unknown SHF

inversely using the measured temperature in the rear of a copper plate. The distribution of the estimated temperature curve can be obtained accurately. The EIPM has the properties of rapid tracking and small affection owing to the noise. Most of input estimation researches were using numerical simulation with assumed known conditions. This study will verify the availability of the EIPM by using the copper plate with 4 different thicknesses. These tests are ignited by using the standard black powder heat source from the igniter stick. This study presents an on-line input method to estimate unknown SHF from the transient temperature data measured by a fine gage thermocouple on the outer surface of a copper plate. The influence owing to the processing noise variance Q is investigated to show the robustness and efficiency of the EIPM.

II. METHODS

The standard black powder heat source with SHF of $q(t)$ is applied at $x = 0$. The copper plate is thin enough to assume that it is a homogeneous thermal conductor with thickness L. The boundary condition of $x = L$ is insulated. The temperature is measured using a fine gage K type thermocouple. By equipping the thermocouple sensor at the position $x = L$ and measuring the surface temperature of the copper plate, the heat-conducting model is formed as shown in Fig. 2.

The 1-D heat-conducting governing equations are as follows:

$$k\frac{\partial^2 T}{\partial x^2} = \rho c_p \frac{\partial T}{\partial t} \quad 0 < x < L, 0 < t \le t_f \tag{1}$$

$$-k\frac{\partial T}{\partial x} = q(t) \quad x = 0, t > 0 \tag{2}$$

$$-k\frac{\partial T}{\partial x} = 0 \quad x = L, t > 0 \tag{3}$$

$$T(x,0) = T_0 \quad 0 \le x \le L \tag{4}$$

$$z(t) = T(x,t) + v(t) \quad x = L \tag{5}$$

where T_0 is the initial temperature. $z(t)$ is the temperature measurement. $T(x,t)$ represents that the temperature is a function of time t and the position x. $v(t)$ is the measurement noise which is assumed to be the Gaussian white noise with zero mean. The proportionality constant k is a transport property known as the thermal conductivity ($W/m{\cdot}K$) of a copper plate.

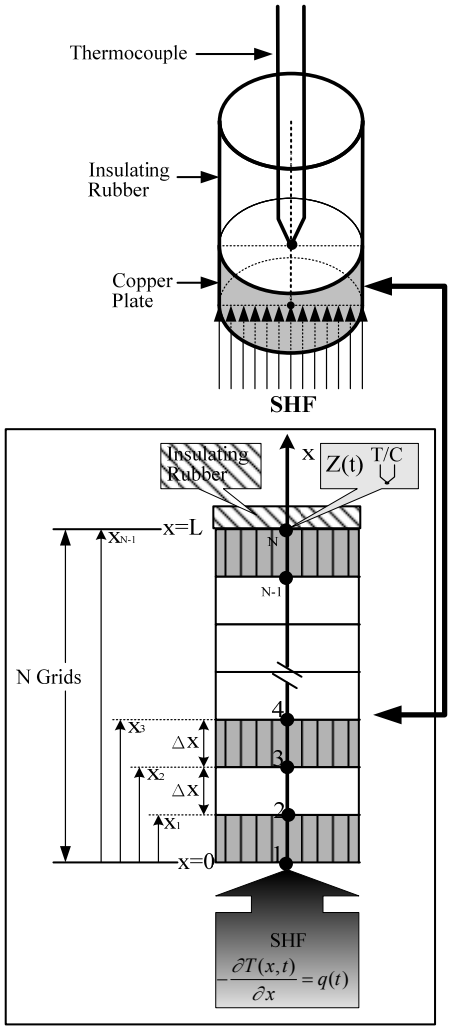

Fig.2. Physical model of one dimensional inverse heat conduction problem (geometry and coordinates).

Density ρ and specific heat c_p are two such properties used extensively in thermodynamic analysis. The product ρc_p ($J/m^3{\cdot}K$), commonly termed the volumetric heat capacity, measures the ability of a material to store thermal energy. The equations (1)~(5) are the heat-conducting governing equations of the copper plate. The equation (5) is the measured equation.

The copper plate is separated into N-1 equal portions with the length of Δx. "$i = 1$" is marked at x=0. The temperature is T_1. "$i = N$" is marked at $x = L$. The temperature is T_N. By using the D`Souza [15] central differential method to substitute Equation (1) in the space derivative and the boundary condition equations, the heat-conducting governing equations can be transferred as following differential equation. The deduced process can be shown as follows:

$$\frac{\partial T_i}{\partial x}=\frac{T_{i+1}-T_{i-1}}{2\Delta x},\frac{\partial^2 T}{\partial x^2}=\frac{T_{i+1}-2T_i+T_{i-1}}{\Delta x^2} \tag{6}$$

when $i=1$

$$\dot{T}_1(t)=\frac{\partial T_1}{\partial t}=\frac{k}{\rho c_p}\frac{\partial^2 T_1}{\partial x^2}=\frac{k}{\rho c_p}\frac{T_2-2T_1+T_0}{\Delta x^2} \tag{7}$$

From the boundary condition in equation (2), it is clear that

$$-k\frac{\partial T_1}{\partial x}=-k\frac{T_2-T_0}{2\Delta x}=q(t) \tag{8}$$

$$T_0=T_2+\frac{2q(t)\Delta x}{k} \tag{9}$$

By substituting equation (9) to (7) can be rearranged as follows:

$$\dot{T}_1(t)=\frac{2k(T_2-T_1)}{\rho c_p\Delta x^2}+\frac{2q(t)}{\rho c_p\Delta x} \tag{10}$$

when $i=2,3,\ldots,i,\ldots,N$ can be obtained as the following equation.

$$\dot{T}_i(t)=\frac{k}{\rho c_p}\left(\frac{T_{i+1}-2T_i+T_{i-1}}{\Delta x^2}\right) \tag{11}$$

when $i=2,3,\cdots N$, the equation (11) can be rearranged as follows:

$$\dot{T}_i(t)=\frac{k}{\rho c_p\Delta x^2}(T_{i+1}-2T_i+T_{i-1}) \tag{12}$$

when $i=N$, the equation (11) can be rearranged as follows:

$$\dot{T}_N(t)=\frac{k}{\rho c_p\Delta x^2}(T_{N+1}-2T_N+T_{N-1}) \tag{13}$$

From the boundary condition in equation (5), it is clear that

$$-k\frac{\partial T_N}{\partial x}=-k\frac{T_{N+1}-T_{N-1}}{2\Delta x}=0 \tag{14}$$

$$T_{N+1}=T_{N-1} \tag{15}$$

By substituting equation (15) to (13) can be rearranged as follows:

$$\dot{T}_N(t)=\frac{2k}{\rho c_p\Delta x^2}T_{N-1}-\frac{2k}{\rho c_p\Delta x^2}T_N \tag{16}$$

From the equations (10-12, 15) and the fictitious process noise input, the one-dimensional continuous-time state equation can be obtained as the following:

$$\dot{T}(t)=AT(t)+Bq(t)+Cw(t) \tag{17}$$

$$T(t)=\{T_1(t),T_2(t),\ldots,T_N(t)\}^T \tag{18}$$

Let $\alpha=\frac{k}{\rho c_p\Delta x^2}$, then, the state matrix, A is shown as follows:

$$A=\begin{bmatrix}
-2\alpha & 2\alpha & 0 & \cdots & & & 0 & \cdots & & \cdots 0\\
\alpha & -2\alpha & \alpha & 0 & \cdots & & \cdots & & & \cdots 0\\
0 & \alpha & -2\alpha & \alpha & 0 & \cdots & 0 & \ldots & & \cdots 0\\
\vdots & & \ddots & \ddots & & & & & & \\
0 & \ldots & & \alpha & -2\alpha & 0 & 0 & 0 & \cdots & \cdots 0\\
\vdots & & \cdots & 0 & \alpha & -2\alpha & 0 & 0 & \cdots & \cdots 0\\
 & & \cdots & 0 & 0 & \alpha & -2\alpha & 0 & \cdots & \cdots 0\\
\vdots & & \cdots & & & 0 & \alpha & -2\alpha & 0 & \cdots 0\\
0 & 0 & & \cdots & & \ddots & \ddots & \ddots & \ddots & \cdots 0\\
0 & 0 & \cdots & & & 0 & \cdots & 0 & 2 & -2\alpha
\end{bmatrix} \tag{19}$$

$$B=\begin{bmatrix}\frac{2}{\rho c_p\Delta x}\\0\\0\\\vdots\\0\end{bmatrix} \tag{20}$$

where A is the state matrix, B and C are the input matrices. $w(t)$ is assumed to be the Gaussian white noise with zero mean and it represents the modeling error. The continuous-time state equation (17) can be discretized with the sampling time Δt. The discrete-time state equation and its relative equations are shown as follows:

$$T(k+1)=\Phi[(k+1)\Delta t,k\Delta t]T(k)+\Gamma(k+1)q(k)+w(k+1) \tag{21}$$

where

$$\Phi[(k+1)\Delta t,k\Delta t]=e^{A\Delta t}$$

$$\Gamma(k+1)=\int_{k\Delta t}^{(k+1)\Delta t}\Phi[(k+1)\Delta t,\tau]B(\tau)d\tau$$

$$w(k+1)=\int_{k\Delta t}^{(k+1)\Delta t}\Phi[(k+1)\Delta t,\tau]G(\tau)w(\tau)d\tau$$

$w(k)$ is the processing error input vector assumed to be the Gaussian white noise with zero mean and with the variance $E\{w(k)w^T(j)\}=Q\delta_{kj}$. δ_{kj} is the Dirac delta function. The discrete-time measurement equation is shown below.

$$z(k)=HT(k)+v(k) \tag{22}$$

where $Z(k)$ is the observation vector at the kth sampling time. $H=[0\ 0.....1]$ is the measurement matrix. $v(k)$ is the measurement error vector assumed to be the Gaussian white noise with zero mean and with the

variance $E\{v(k)v^T(j)\} = R\delta_{kj}$.

The EIPM has two parts: one is the Kalman filter without the input term and the other is the fuzzy weighted recursive least square estimator. The system input is the unknown SHF. The Kalman filter is operating under the setting of the processing error variance Q and the measurement error variance R. It is to use the difference between the measurements and the estimated values of the system temperature as the functional index. Furthermore, by using the recursive least square estimator, the SHF can be precisely estimated.

The equations of the Kalman filter are shown as follows [16]:

$$\bar{X}(k/k-1) = \Phi\bar{X}(k-1/k-1) \quad (23)$$

$$P(k/k-1) = \Phi P(k-1/k-1)\Phi^T + Q \quad (24)$$

$$s(k) = HP(k/k-1)H^T + R \quad (25)$$

$$K(k) = P(k/k-1)H^T s^{-1}(k) \quad (26)$$

$$P(k/k) = [I - K(k)H]P(k/k-1) \quad (27)$$

$$\bar{Z}(k) = Z(k) - H\bar{X}(k/k-1) \quad (28)$$

$$\bar{X}(k/k) = \bar{X}(k/k-1) + K(k)\bar{Z}(k) \quad (29)$$

The recursive least square estimator:

$$B(k) = H[\Phi M(k-1) + I]\Gamma \quad (30)$$

$$M(k) = [I - K(k)H][\Phi M(k-1) + I] \quad (31)$$

$$K_b(k) = \gamma^{-1}P_b(k-1)B^T(k)\left[B(k)\gamma^{-1}P_b(k-1)B^T(k) + s(k)\right]^{-1} \quad (32)$$

$$P_b(k) = \left[I - K_b(k)B(k)\right]\gamma^{-1}P_b(k-1) \quad (33)$$

$$\hat{q}(k) = \hat{q}(k-1) + K_b(k)\left[\bar{Z}(k) - B(k)\hat{q}(k-1)\right] \quad (34)$$

$$\hat{X}(k/k-1) = \Phi\hat{X}(k-1/k-1) + \Gamma\hat{q}(k) \quad (35)$$

$$\hat{X}(k/k) = \hat{X}(k/k-1) + K(k)\left[Z(k) - H\hat{X}(k/k-1)\right] \quad (36)$$

where P is the filtering error covariance matrix. $s(k)$ is the residual covariance. $\bar{Z}(k)$ is the bias innovation produced by the measurement noise and the input disturbance. $B(k)$ and $M(k)$ are the sensitivity matrices. $K_b(k)$ is the correction gain. $P_b(k)$ is the error covariance of the estimated input vector. γ is the weighting constant or weighting factor in the range $0 < \gamma \le 1$. $\hat{q}(k)$ is the estimated input vector. After the state equation is obtained, the inverse estimation process is carried out using the EAIEM system based on the Kalman filter and the recursive least squares estimation algorithm.

Ⅲ. EXPERIMENTAL METHODS

The purpose of experiment is to inversely estimate the temperature and SHF of the igniter stick by using the temperature measurements of the copper plate surface. The entire experiment modular includes the impulse heat source, the sensor, the high-speed data acquisition device, and the computer module. The copper plate is heated by adopting the standard impulse heat source and the fine gage K type thermocouple is set in the rear of the thin copper plate. The DAQ is linked with the thermocouple to measure the temperature data. In the SHF for explosives, the measurement method must cope with rapidly changing burning chiefly with the transient temperature measurements. The experiment devices and the elements (Fig. 3) used are illustrated as follows:

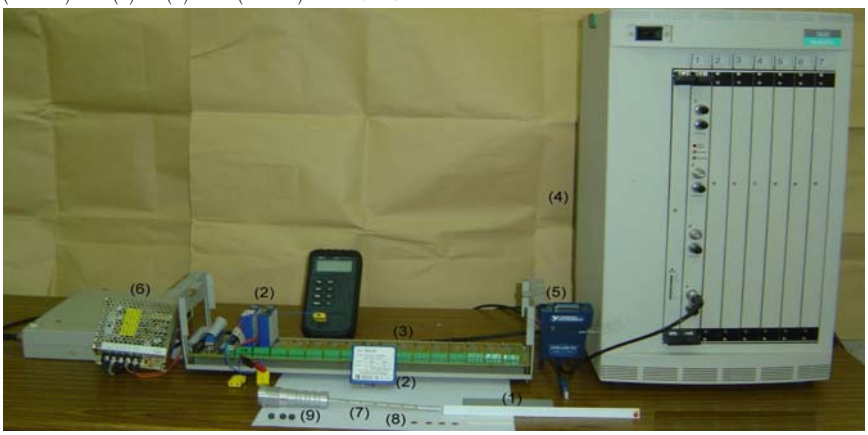

(1) The fine gage K type thermocouple: 

Fig.3. Diagram of the experimental facility: (1) The fine gage K type thermocouple, (2) The 5B40 wide bandwidth voltage input module, (3) The 5B16B 16-channel back panel, (4) Nicolet MultiPro 120, High-speed DAQ, (5) GPIB Controller for Hi-Speed USB, (6) +5VDC power, (7) A igniter stick, (8) Copper plates, L=0.15, 0.20, 0.25, and 0.30 mm, (9) Three pellets of black powder.

Sensors

A thermocouple is created whenever two dissimilar metals touch and the contact point produces a small open-circuit voltage as a function of temperature. The fine gage K type thermocouple has one nickel-chromium alloy conductor and one nickel-aluminum alloy conductor. Thermocouples require some form of temperature reference to compensate for these implementing cold-junction compensation: hardware compensation and software compensation. Both techniques require that the temperature at the reference junction be sensed with a direct-reading sensor. We used fine gage K type thermocouples whenever fast, accurate temperature measurements were required. The fine wire diameters enable accurate temperature measurements without disturbing the base temperature of the body by keeping heat transfer via the leads to a minimum. They are available in wire sized 0.125 mm in diameter. To insure consistent thermoelectric properties, the fine gage thermocouples are made from carefully selected materials, made from matched wire pairs within the same lot number.

Signal conditioning modules

The signals of thermocouple output are typically in the mV range, making them susceptible to noise. Thermocouples generate signals too small to measure directly with a DAQ device. When dealing with small voltages, noisy environments, extreme low signals, or simultaneous signal measurement, signal conditioning is essential for an effective DAQ system. Signal conditioning maximizes the accuracy of a system, allows sensors to operate properly, and guarantees safety. It is important to select the right hardware for signal conditioning. Signal conditioning is offered in modular.

The 5B40 wide bandwidth voltage input module provides a single channel of analog input which is amplified, isolated and converted into high-level analog voltage output. This voltage output is logic-switch controlled, allowing these modules to share a common analog bus without the need for external multiplexers. The input signal is processed through a pre-amplifier on the field side of the isolation barrier. This pre-amplifier has a gain-bandwidth product of 5MHz and is bandwidth limited to 10 kHz. After amplification, the input signal is chopped by a proprietary chopper circuit. Isolation is provided by a transformer coupling, again using a proprietary unwanted parasitic cold junctions. The most common method is to measure the temperature at the reference junction with a direct-reading temperature sensor and subtract the parasitic junction voltage contributions. This process is called cold-junction compensation. The measured voltage is in fact independent of the composition of the measurement leads and the cold junctions. There are two techniques for technique to suppress common mode spike or surge transmission. This module is powered from +5VDC, ±5%. The 5B16B 16-channel back panel which has 16 non-addressable analog I/O signal channels and includes on-board temperature sensors and cold junction compensation (CJC), power supplies, mounting racks, interface cables and evaluation boards, accepts the 5B analog modules in any mixture.

High-speed DAQ Hardware

Nicolet MultiPro 120 (MP) acts as the interface between the computer and the outside world. It functions primarily as a device that digitizes incoming analog signals so that the computer can interpret them. Its functions include a combination of analog, digital and counter operations on a single device for powerful transient measurement. MP complies with the IEEE-488.2 standard for convenient interface with GPIB instruments.

The computer module (including the software programs):

(1) Intel processor 1.6G computer, the signal software, and the Matlab programming language can be used to process the signal data.

(2) The Team 256 acquisition software:

The application software of Team 256 adds analysis and presentation capabilities to the driver software. The Team 256 in coordination with the data acquisition system can collect data from the subject system in real time. The sampling rate, the temperature range, the sampling time, the frequency channel, and the record style to record the real-time signal of the system can be configured. Team 256 is an easy-to-use yet very flexible tool specifically designed for data logging applications. With intuitive dialog windows, it can configure our logging task to easily acquire, log, view and share data. It is a stand-alone and configuration-based data logging software.

(3) The EIPM can be programmed by using the Matlab programming language. The

temperature measurements are then regarded as the inputs into the EIPM which is to estimate the SHF in the front of the copper plate.

Ⅳ. RESULTS AND DISCUSSIONS

To verify the estimated performance of the EIPM, an inverse heat conduction problem of the copper plate is considered. The SHF in the front and temperature are estimated inversely by measuring the temperature in the rear. The test is heated by the standard impulse heat source with the fixed power (three black powder pellets: KNO_3, 74% ; Sulfur, 10.4%; Charcoal, 15.6%). The rear of the copper plate is insulated with the insulating rubber. The transient temperature data are measured using a fine gage K type thermocouple in the rear of the copper plate whose 4 different thicknesses are 0.15 mm, 0,20 mm, 0.25 mm, and 0.30 mm. Using a total time period of t_f =1 sec and a sampling interval of Δt =0.0005 sec (20 kHz), find the measurement temperature curves of 4 different tests shown in Fig. 4. It shows that the measurement error of

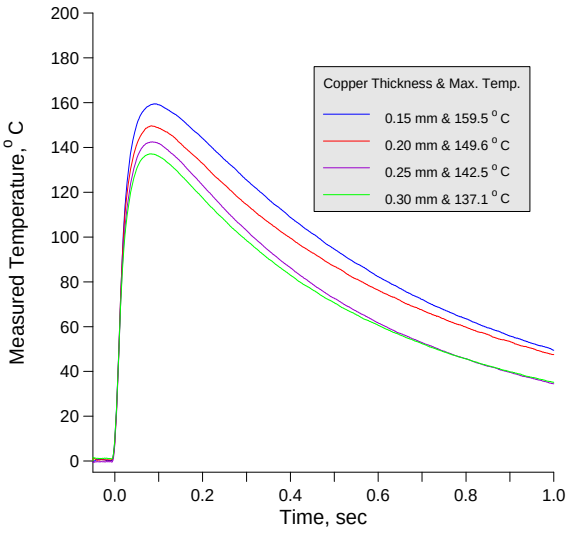

Fig.4. Experimentally measured temperature-time curves at x=L for properly ignited three pellets of black powder.

the thermocouple is approximately ±0.01% (with the measurement noise covariance, $R=10^{-4}$).

Using the space interval of $\Delta x = L/10$, the processing noise covariance matrix of $Q=10^3$ and the measured temperatures in the rear of different samples with 4 different thicknesses (L=0.15, 0.20, 0.25 and 0.30 mm), SHF vs. time (Fig. 5(a)~(d)) may be obtained from Fig.4. Fig. 5 shows that the SHF in the front is estimated inversely by substituting the temperature data into the EIPM. The max. SHF values are 19324, 19439, 19194, and 19101 kW/m^2, respectively. The estimation results demonstrate that the penetration delay of temperature does not exist in the estimation process. The standard black powder heat source is in an absolutely insulated condition in the measurement process, in order to reduce the influence of the penetration delay of temperature, the max. values and shapes of impulse curves are showed clearly to verify the

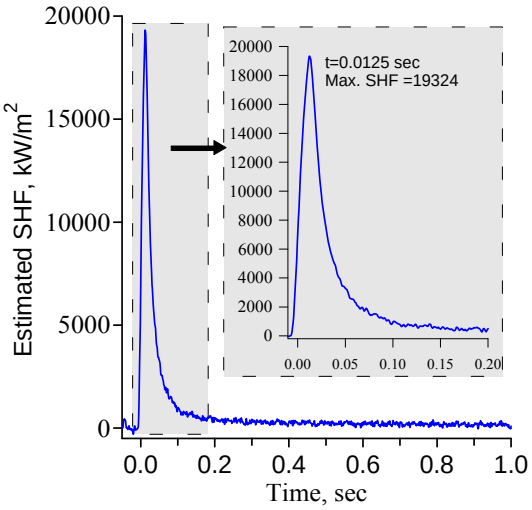

(a) The estimated SHF (L=0.15 mm).

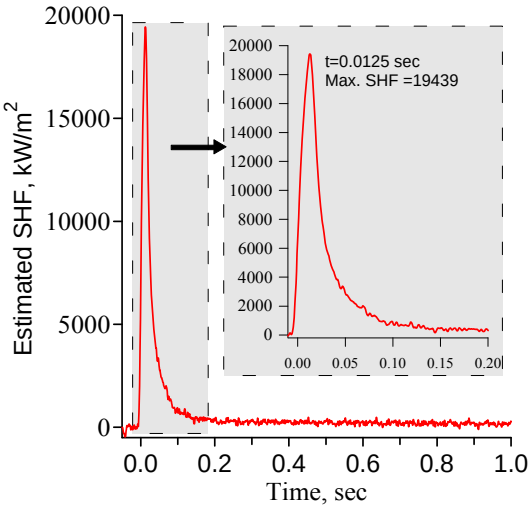

(b) The estimated SHF (L=0.20 mm).

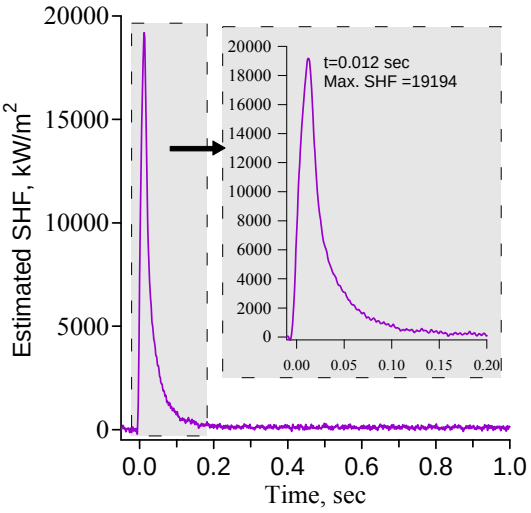

(c) The estimated SHF (L=0.25 mm).

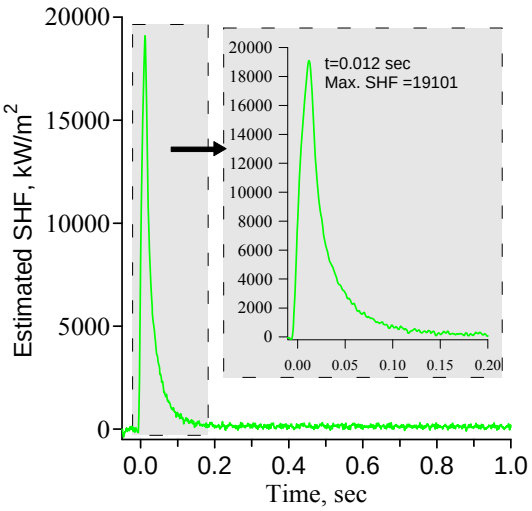

(d) The estimated SHF (L=0.30 mm).

Fig.5. Estimated SHF–time curve at x=0 by EIPM with measured temperature in Fig. 4 as input.

accuracy of the EIPM. Fig. 5(a)~(d) look very much alike and are in good agreement. Therefore, it appears that the estimated SHF is the heat flux generated by the igniter stick on the copper plate front.

Fig. 6 shows the increasing modeling error as $Q=10^{-1}$, 10^{3}, and 10^{6}. The Kalman filter is operating under the setting of the processing error variance Q and the measurement error variance R. It regards the renewal values produced by using the difference between the temperature estimates and the temperature measurements as the functional index, and utilizes the real-time least square algorithm to precisely estimate the SHF. The measurement error variance of the thermocouple is assumed as

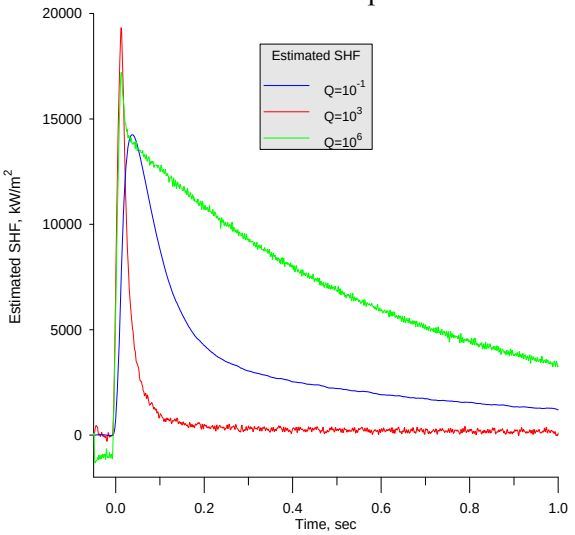

Fig.6. Estimated SHF curves at x=0 by means of EIPM with the processing noise variance of $Q=10^{-1}$, 10^{3}, and 10^{6} as input.

a given value $R=10^{-4}$. The processing error variance Q is adjusted between 10^{-1} to 10^{6}. The temperature measurements are then regarded as the inputs into the EIPM which estimates the SHF in the rear of the copper plate, *L=0.15* mm. When the processing noise variance Q increases, it will accelerate the estimation speed and produce the better estimation result. When the processing noise variance Q decreases, the error covariance matrix will decrease and the Kalman gain $K(k)$ will decrease. The main reason is that the correction need is decreasing and the smaller Kalman gain $K(k)$ is needed to offer that correction. When the processing noise variance Q increases, the error covariance matrix will increase. The main reason is that the correction need is increasing and the larger Kalman gain $K(k)$ is needed to offer that correction. As a result, the Kalman filter will have faster correction performance but have larger oscillation in the estimation process. When the processing noise variance Q increases ($Q=10^{-1}\sim 10^{3}$), the EIPM makes the new measurement significant for the correction of estimation. The relative root mean square error is reduced. If the modeling error is too large ($Q=10^{6}$), the Kalman filter will produce larger oscillations which cause the increase of the relative root mean square error value. As a result, the relatively smaller value of relative root mean

square error is making the parameter $Q=10^3$ the most excellent option. $Q=10^{-1}$, 10^3, and 10^6 in Fig. 6 are used to show that when the error is larger, the result with the larger oscillation and faster response will be produced. The processing noise variance of $Q=10^{-1}$ in Fig. 7 shows that the estimated temperature curve can't be estimated accurately.

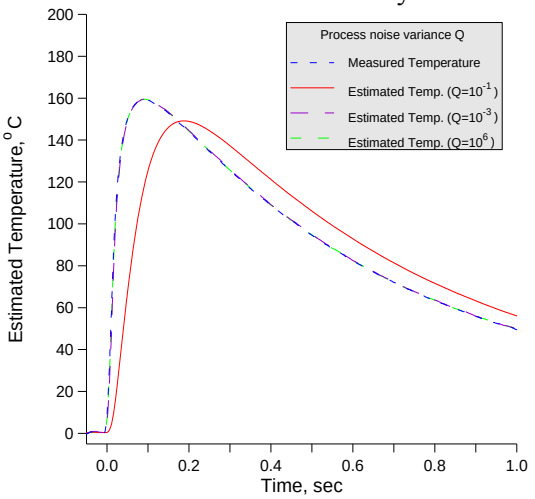

Fig.7. Estimated temperature-time curve at x=L by direct heat conduction problem with estimated SHF in Fig. 6 as input.

V. CONCLUSIONS

The fronts of the copper plate samples with 4 different thicknesses are heated by applying the standard superquick heat source and the temperatures in the rears are measured by using the fine gage K type thermocouples. The EIPM, including the extended Kalman filter and on-line input estimation, can accurately and efficiently estimate the SHF inside explosives in real time and produce a rapid reaction speed when the length of the sampling time is very short. The EIPM is utilizing the transient measured temperature data to estimate the SHF in the front of the copper plate at the end of the igniter stick. The influence on the estimation caused by the processing noise variance Q is investigated by utilizing the experimental verification. The results reveal that if the processing noise variance Q increases, the faster estimation convergence and larger oscillations will be produced. The experimental verification shows that the EIPM has the properties of better targat tracking capability and more effective noise reduction, and that it is an efficient inverse estimation method for the estimation of the unknown SHF of the igniter stick.

SYMBOLS

B	sensitivity matrix
c_p	specific heat at constant pressure, $J/kg{\cdot}K$
D	coefficient matrix
H	measurement matrix
h	convection heat transfer coefficient, $W/m^2{\cdot}K$
I	identity matrix
$K(k)$	Kalman gain
K	time step (discretized)
k	thermal conductivity of a copper plate, $W/m{\cdot}K$
M	sensitivity matrix
N	total number of nodes
P	filtering error covariance matrix
P_b	error covariance matrix
q	heat flux, W/m^2
s	residual covariance
$s(k)$	innovation covariance matrix
T	temperature, ℃
t	time, sec
P	measurement noise variance
Q	processing noise variance
v	measurement noise vector
$z(t)$	measured temperature, ℃

Greek Letters

α	thermal diffusivity
Γ	input matrix
γ	weighting factor
Δt	sampling interval
δ	Dirac delta function
v	measurement noise vector
ρ	copper density , kg/m^3
Φ	state transition matrix

Ω coefficient matrix

Ψ coefficient matrix

Superscripts

^{T} transpose of the matrix

' fluctuating quality

Overbar

$\bar{}$ dimensionless

^ estimated value

REFERENCES

[1] Silva Neto, A. J. and Ozisik, M. V., "Simultaneous Estimation of Location and Timewise-Varying Strength of a Plane Heat Source," Numerical Heat Transfer, Part A, Vol. 24, pp. 467-477, 1993.

[2] Lee, W. S., Ko, Y. H., and Ji, C. C., "A Study of an Inverse Method for the Estimation of Impulsive Heat Flux," J. Franklin Inst., Vol. 337, No. 6, pp. 661-671, 2000.

[3] Chen, T. C. and Tuan, P. C., "Input Estimation Method Including Finite-Element Scheme for Solving Inverse Heat Conduction Problems," Numerical Heat Transfer, Part B, Vol. 47, pp. 1-14, 2005.

[4] Yu, G. H. "A Study of the Thermal Conductive Behaviors of Composite Materials with Double Layers," Department of Construction Engineering, National Kaohsiung First University of Science and Technology, Master Paper, 2004.

[5] Hon, R. L. "A Study of the Thermal Conductive Behaviors of Double Composite Layers with Constant Heat," Department of Construction Engineering, National Kaohsiung First University of Science and Technology, Master Paper, 2006.

[6] Huang, C. H. and Ozisik, M. N., "Inverse Problem of Determining Unknown Wall Heat Flux in Laminar Flow Through a Parallel Plat Duct," Numerical Heat Transfer, Part A, Vol. 21, pp. 55-70, 1992.

[7] Li, H. Y. and Yan, W. M., "Inverse Convection Problem for Determining Wall Heat Flux in Annular Duct Flow," Journal of Heat Transfer Transactions of the ASME, Vol. 122, pp. 460-464, 2000.

[8] Meng, H. H., Aircraft Maneuver Detection Using an Adaptive Kalman Filter, Master's Thesis, Naval Postgraduate School, Monterey, California, USA., 1989.

[9] Scarpa, F. and Milano, G., "Kalman Smoothing Technique Applied to the Inverse Heat Conduction Problem," Numerical Heat Transfer. Part B, Vol. 28, pp. 79-96, 1995.

[10] Polat, S., Mujumdar, A. S., Heiningen, A. R. P., and Douglas, W. J. M., "Numerical Model for Turbulent Jet Impinging on a Surface with Through-Flow," Int. J. Thermophysics, Vol. 5, No. 2, pp. 172-180, 1991.

[11] Linton, R. L. and Agonafer, D., "Coarse and Detailed CFD Modeling of a Finned Heat Sink," IEEE Transactions on Components Packaging and Manufacturing Technology A, Vol. 18, No. 3, pp. 517-520, 1995.

[12] Sathe, S., Kelkar, K. M. K., Karki, C., Tai, C., Lamb, C., and Patankar, S. V., "Numerical Prediction of Flow and Heat Transfer in an Impingement Heat Sink," Journal of Electronic Packaging, Vol. 119, No. 1, pp. 58-63, 1997.

[13] Jonsson, H. and Palm, B., "Thermal and Hydraulic Behavior of Plate Fin and Strip Fin Heat Sinks Under Varying Bypass Conditions," IEEE Transactions on Components and Packaging Technologies, Vol. 23, No. 1, pp. 47-54, 2000.

[14] Maveety, J. G. and Jung, H. H., "Design of an Optimal Pin-Fin Heat Sink with Air Impingement Cooling," International Communication on Heat and Mass Transfer, Vol. 27, No. 2, pp. 229-240, 2000.

[15] D'Souza, N. "Numerical Solution of One-dimensional Inverse Transient Heat Conduction by Finite Difference Method," ASME Paper 75-WA/HT-81, 1975.

[16] 陳新海，最佳估計理論，北京航空學院出版社，北京，第184-201頁，1987。